Supplementary Information (SI) for ChemComm.
This journal is © The Royal Society of Chemistry 2024

Supplementary Information

Porphyrin-silver acetylide cluster catalysts with dual active sites for the electrochemical reduction of CO2

Leonard Curet,[a] *Dominique Foix,* [a] *Emilio Palomares,* [b,c] *Laurent Billon,* [a] *Aurelien Viterisi,**[a]

[a] Universite de Pau et Pays de l'Adour, E2S UPPA, CNRS, IPREM UMR 5254

Technopole Hélioparc

2 avenue du Président Pierre Angot

64053 PAU CEDEX 09

[b] Institute of chemical research of Catalonia (ICIQ)

Avda. Països Catalans, 16

43007 Tarragona

[d] ICREA. Passeig Lluís Companys, 28, E-08010. Barcelona. Spain.

* aurelien.viterisi@univ-pau.fr

Experimental section

Materials

25% ammonia solution (for analysis EMSURE® ISO, Reag. Ph Eur), silver nitrate (ReagentPlus®, ≥99.0% for titration), $FeBr_2$ (98%), Cobalt(II) acetate tetrahydrate (ACS reagent, ≥98.0%),Benzaldehyde (ReagentPlus®, ≥99%), Pyrrole (for synthesis), Boron trifluoride diethyl etherate (for synthesis), DDQ (98%), TBAF solution (1.0 M in THF), DIPEA (ReagentPlus®, ≥99%), 2,6-lutidine (ReagentPlus®, ≥98%), absolute ethanol, Nafion© perfluorinated resin (5 wt% solution in a mixture of lower aliphatic alcohols containing 5% water), DMF (anhydrous, 99.8%), Graphiteand potassium bicarbonate (ACS reagent, 99.7%, powder, crystals, or granules) were purchased from Sigma-Aldrich. 4-(Trimethylsilyl)ethynylbenzaldehyde (95%) was purchased from Manchester organics. Sigracet GDL (39BB) was purchased from Fuel Cell Store. CDCl3 (99.8%) was purchased from Innovachem. Biobeads SX-3 was purchased from Bio-Rad Laboratories. All electrolytes were prepared using Milli-Q water. All solvents were of HPLC grade or higher. Dry DCM was purified on a SPS.

Materials characterization

NMR

The ^{1}H-NMR analyses were conducted using a Bruker Ultrashield spectrometer with a ^{1}H frequency of 400 MHz.

SEM-EDX

Scanning electron microscopy (SEM) was performed on an APREO 2 SEM (Thermo-Fisher Scientific) with an EDX XFlash 6-100 (Brüker) for qualitative and quantitative elemental measurements. Measurements were done using a 2.00 kV accelerating Voltage and 25pA for the beam current.

XPS

X-ray Photoelectron Spectroscopy (XPS) measurements were carried out with a THERMO Escalab 250Xi spectrometer, using focused monochromatic Al Kα radiation (hν = 1486.6 eV) with an Xray spot size of 650µm for longer axis ellipse. The high-energy resolution spectra were recorded with constant pass energy of 20 eV. The charge neutralization was used for all the acquisitions. The pressure in the analysis chamber was around 2×10^{-7}mbar during analysis. Lower resolution spectra were recorded with short acquisition times before each experiment to check that the samples were not subject to degradation during the X-ray irradiation. The binding energy scale was calibrated using the C1s peak at 285.0 eV from the hydrocarbon contamination always present on the samples' surface. For data analysis, the spectra were mathematically fitted using Casa XPS software, employing a least-squares algorithm and a non-linear baseline. The fitting of peaks in the experimental curves was achieved through a combination of Gaussian (70%) and Lorentzian (30%) distributions.

Powder XRD

Powder X-ray Diffraction (PXRD) characterization was performed using a Bruker D2 Phaser powder diffractometer equipped with a Cu Kα radiation source with a wavelength of 1.5406 Å. XRD patterns were recorded in the 2θ range of 10° to 80° with a step size of 0.021° and a counting time of 0.05 seconds per step. The crystallite sizes were determined using DIFFRAC.EVA software.

ATR-IR

ATR-IR characterization was performed on a Nicolet iS50 (Thermo Scientific) with 64 scans.

3-Electrodes Cell Electrochemical Characterization

Electrochemical tests were conducted using a custom-made three-electrode, leak-tight cell. The anode, consisting of a platinum wire, was enclosed in a bridge tube. The cell was filled with 40 mL of a 1 M $KHCO_3$ solution as the electrolyte. The reference electrode employed was an Ag/AgCl electrode immersed in a 3M KCl solution (E_0=0.210 vs NHE). The working electrode was a Gas Diffusion Electrode (GDE) with a surface area of 2 cm², integrated into a support structure, exposing 1 cm² of its surface directly to the electrolyte.

The pH value of the CO_2-saturated electrolyte was measured to be 6.8 before electrolysis. The potentials were measured against Ag/AgCl (3M). iR compensation losses between the working and reference electrodes were measured using electrochemical impedance spectroscopy (EIS). Electrode potential after iR correction converted to the RHE (Reversible Hydrogen Electrode) scale using equation S1. The pH value was measured to be 7.8 for the CO_2 saturated electrolyte and 8.4 when N_2 saturated. The overpotential (η) was calculated according to Eq. **S2**[1].

Before chronoamperometry experiments, the electrolyte underwent a 15 min purge with either N_2 or CO_2 (at a flow rate of 35 mL/min). This purge was carried out using a Mass Flow Controller (MFC) (Bronkhorst EL-FLOW prestige FG-201CV) and constant stirring to eliminate air from both the solution and the cell headspace. Electrochemical tests were carried out using a potentiostat PGSTAT 204 (Metrohm).

$$E\,(RHE) = E\,(Ag/AgCl) + 0.059 * pH + E_0(Ag/AgCl) \qquad \textit{Eq. S1}$$

With $E\,(Ag/AgCl)$ the measured corrected potential, $E^0(Ag/AgCl)$=0.210 V the standard potential at 3M KCl, pH=7.8 in CO_2 saturated 1M $KHCO_3$ solution

$$\eta = E - E^0_{RHE} \qquad \textbf{Eq. S2}$$

With $E^0_{RHE} = -0.075\,V\ for\ the\ CO2\ to\ CO\ reduction\ at\ pH = 7.8$

Faradaic efficiency was obtained by direct quantification of the gas products:

$$Faradaic\ efficency\ (\%) = \frac{Q_{exp}}{Q_{theo}} \times 100 = \frac{z \times n \times F}{Q} \times 100 \qquad \textbf{Eq. S3}$$

Where z is the number of electrons involved in the reaction, n the number of moles of generated product, F the faraday constant and Q the charge passed during the catalytic experiment.

Electrodes preparation

The Electrodes were prepared following a modified procedure from M. Robert et al [16]. Vulcan XC-72 Carbon Black (3 mg) was sonicated in Absolute ethanol (2mL) for 30min. To the slurry was added Nafion© perfluorinated resin (10 µL of a 5 wt% solution in a mixture of lower aliphatic alcohols containing 5% water) and the mixture was sonicated for 30min. To this mixture was added a suspension of the acetylide (0.8 mg) in absolute ethanol (1mL) and the mixture was sonicated for 30min. The suspension was then deposited by dropcasting on a gas diffusion layer (Sigracet 39BB; 2 cm^2) at 80°C. The electrodes were then dried under reduced pressure at 40°C overnight.

Synthesis protocol

C5-5,10,15,20-tetrakis((4-(trimethylsilyl)ethynyl)phenyl)-21H,23H-

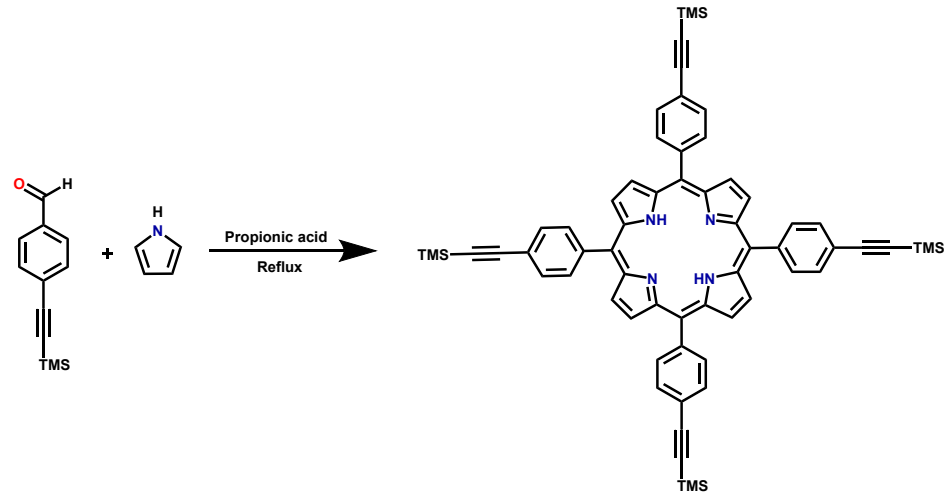

porphyrin

In a 250 mL round flask, 4-((trimethylsilyl)ethynyl)benzaldehyde (4.0443g , 20mmol) in propionic acid (150 mL) was heated at 100°C for 1H. Freshly distilled pyrrole (1.38 mL, 20 mmol) was added dropwise and the solution was refluxed for 3H in the dark. The solvent was evaporated and the residue was purified by crystallization in MeOH. The obtained solid was separated on a column chromatography (silica gel; hexane/DCM 50:50). A second column chromatography (silica gel; hexane/DCM 60:40) was used to obtain the purified product as a purple powder (555 mg; 11% yield; 555 µmol).

^{1}H NMR (400 MHz) $CDCl_3$: 8.81 (s, 8H) ; 8.14 and 7.87 (dd, 16H, J=8.2) ; 0.38 (s,36H) ; -2.84 (s, 2H)

C6 5,10,15,20-tetrakis((4-ethynyl)phenyl)-21H,23H-porphyrin

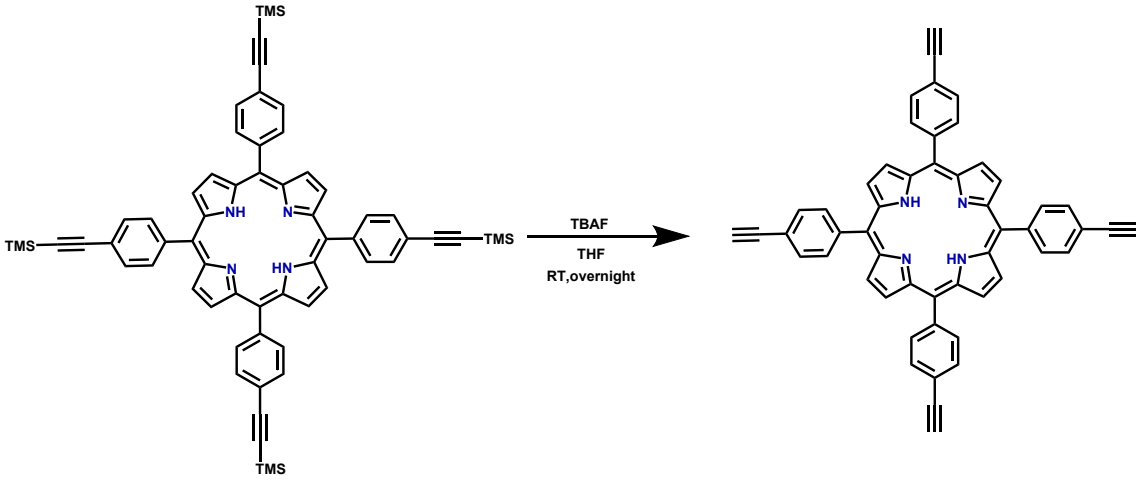

To a solution of LC020 (152.4mg; 152.5µmol) in THF (60 mL) at 0°C was added TBAF (0.8mL; 0.8mmol; 6eq). The mixture was stirred at RT overnight. The solvent was evaporated and the crude material was purified by silica gel chromatography. The solvent was evaporated and the product **C6** was recovered as a purple solid (105.4mg ;148 µmol; 97% yield).

Solubility: DCM, Chloroform, THF, DMF

^{1}H NMR (400 MHz) $CDCl_3$: 8.83 (s, 8H) ; 8.17 and 7.88 (dd,16H, J=8.0) ; 3.32 (s, 4H) ; -2.83 (s, 2H)

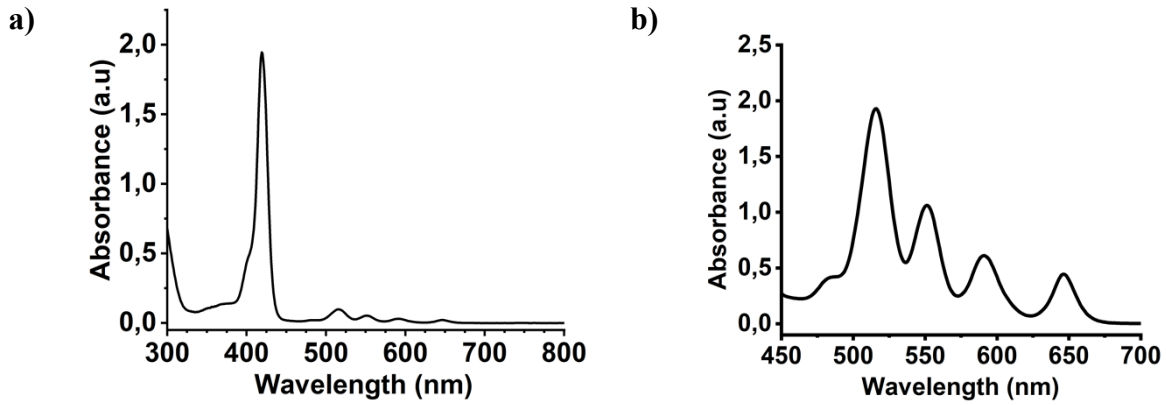

Figure S1 a) UV spectrum of a 10^{-6} M solution of C6 in DCM **b)** UV spectrum of a 10^{-4} M solution of C6 in DCM. Soret: 419 q bands: 516, 551, 591, 646

C7 Iron (III) 5,10,15,20-tetrakis((4-ethynyl)phenyl)-21H,23H-porphyrin chloride

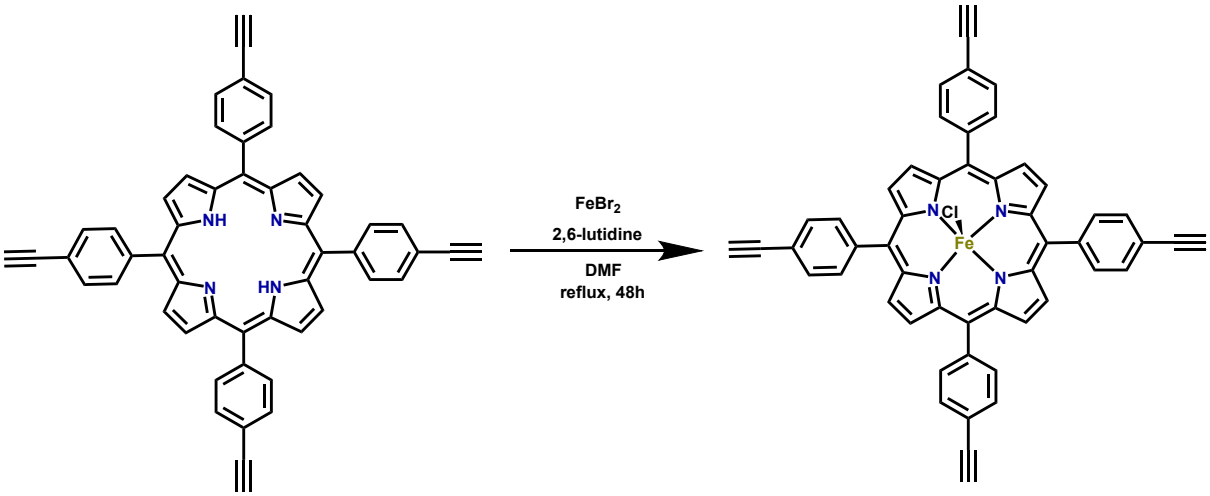

A solution of **C6** (100 mg ; 141µmol ; 1eq), $FeBr_2$ (303 mg ; 1.41mmol ; 10eq) and 2,6-lutidine (33 µL; 281µmol ; 2eq) in DMF (20 mL) was refluxed for 24H under N_2. The material was precipitated by adding an acidic (HCl 1M) solution (50 mL) and washed with distilled water until neutral pH. The obtained solid was purified by column chromatography (silica gel, DCM:MeOH 0 to 20%) and preparative SEC to obtain **C7** (93.2 mg; 116 µmol; 83% yield)

Solubility: DCM, Chloroform, THF, DMF

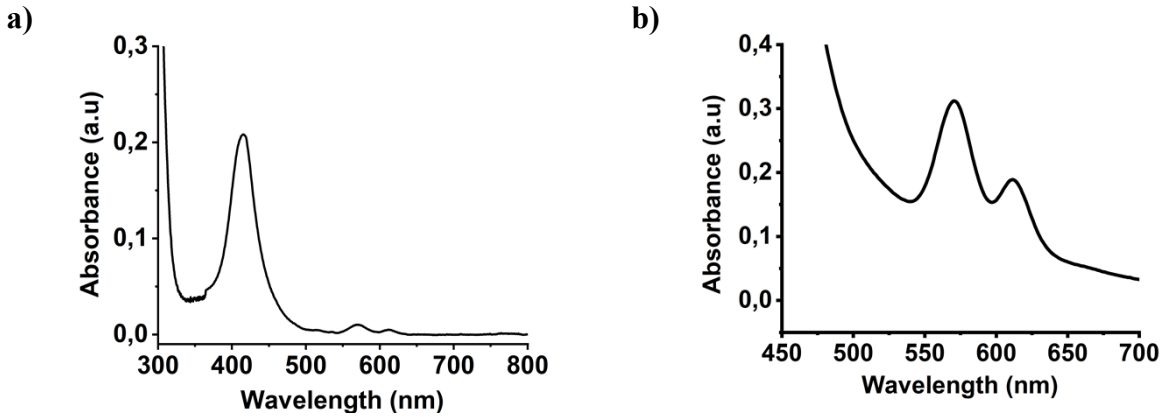

Figure S2 a) UV spectrum of a 10^{-6} M solution of C7 in DCM **b)** UV spectrum of a 10^{-4} M solution of C7 in DCM. Soret: 416; q bands: 571, 612

C8 Cobalt (II) 5,10,15,20-tetrakis((4-ethynyl)phenyl)-21H,23H-porphyrin

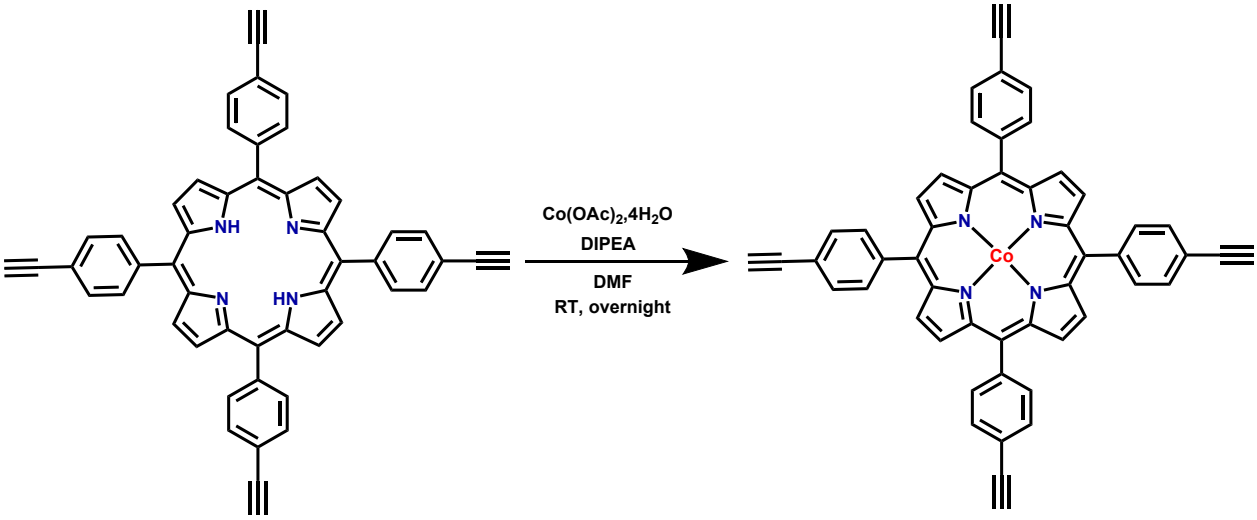

$Co(OAc)_2 \cdot 4H_2O$ (74,5mg, 500µmol; 4eq) was added to a solution of C6 (50mg ; 70,4 µg; 1eq) in DMF (10 mL). DIPEA was added (20µL; 114µmol; 1,5eq) and the mixture was stirred at RT overnight. Water was then added and the precipitate was washed with water solubilised in DCM: hexane (1:1) and purified by column chromatography using a DCM: hexane (1:1) mixture. The solvents were evaporated the obtained C8 dark purple powder was dried under vacuum (52mg; 68 µmol; 96%).
Solubility: DCM, Chloroform, THF, DMF

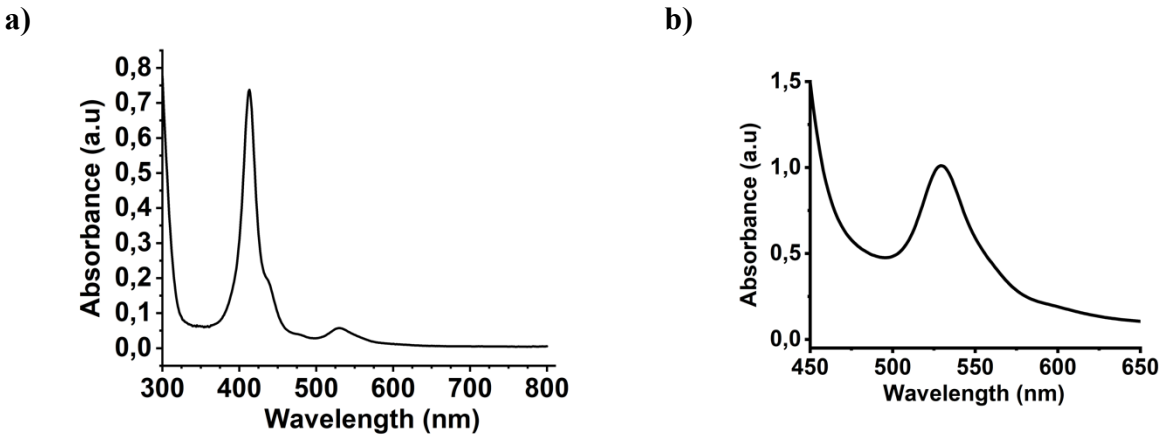

Figure S3 a) UV spectrum of a 10^{-6} M solution of C8 in DCM **b)** UV spectrum of a 10^{-4} M solution of C8 in DCM. Soret: 413 q bands: 531

C9 $[Ag\text{-}FeTaTPP]_x$

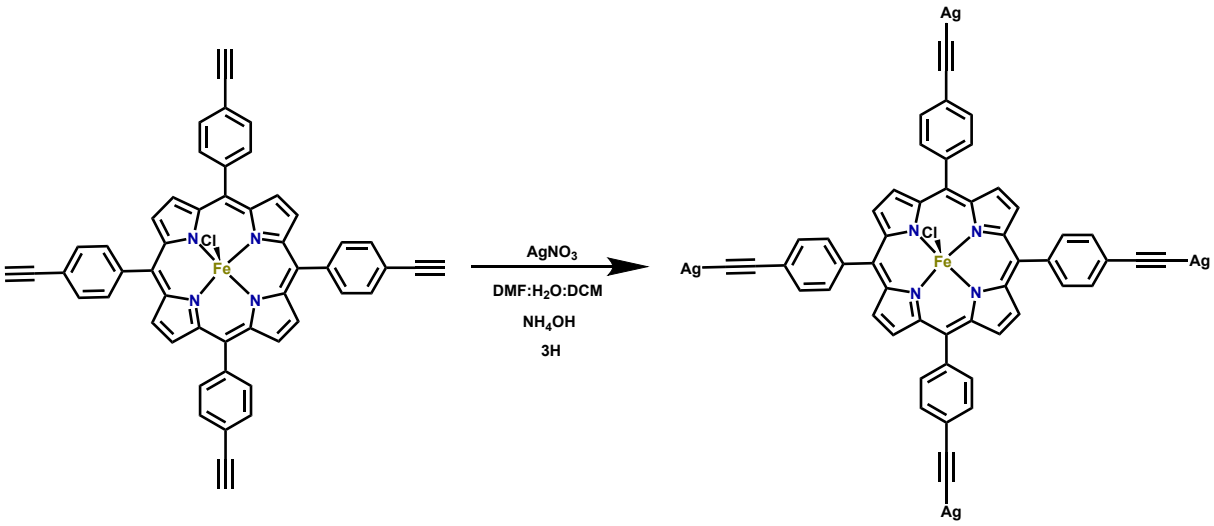

$AgNO_3$ (203.3 mg 1.20 mmol; 10 eq) was solubilized in a mixture of MeOH (10 mL) and water (5 mL). To this solution was added NH_4OH until the brown color completely disappeared. FeTATPPCl (100mg; 120 µmol; 1eq) was dissolved in a mixture of DMF (10mL) and DCM (15mL) and added slowly to the mixture. A precipitate started to form after 10 min and the reaction mixture was stirred at RT for 3H. The solution was filtered and the obtained solid was washed with DMF, water, THF, MeOH and DCM. The resulting dark green solid was obtained quantitatively and dried under high vacuum with phosphorus pentoxide overnight.

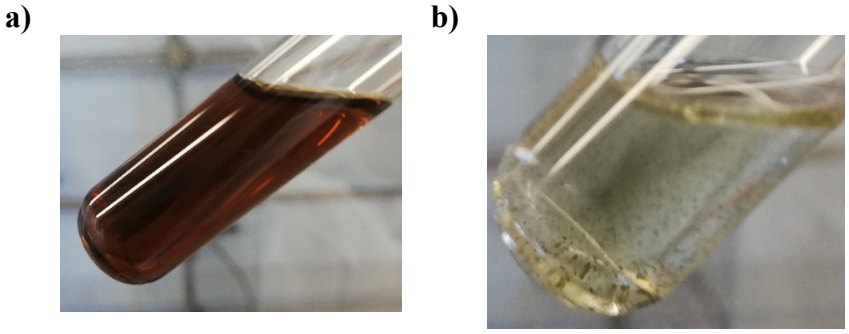

Figure S4 a) C7 solubilised in DCM b) C9 solubilised in DCM. A loss of solubility is observed upon silver addition indicative of the complex formation.

C10 [Ag-CoTaTPP]$_x$

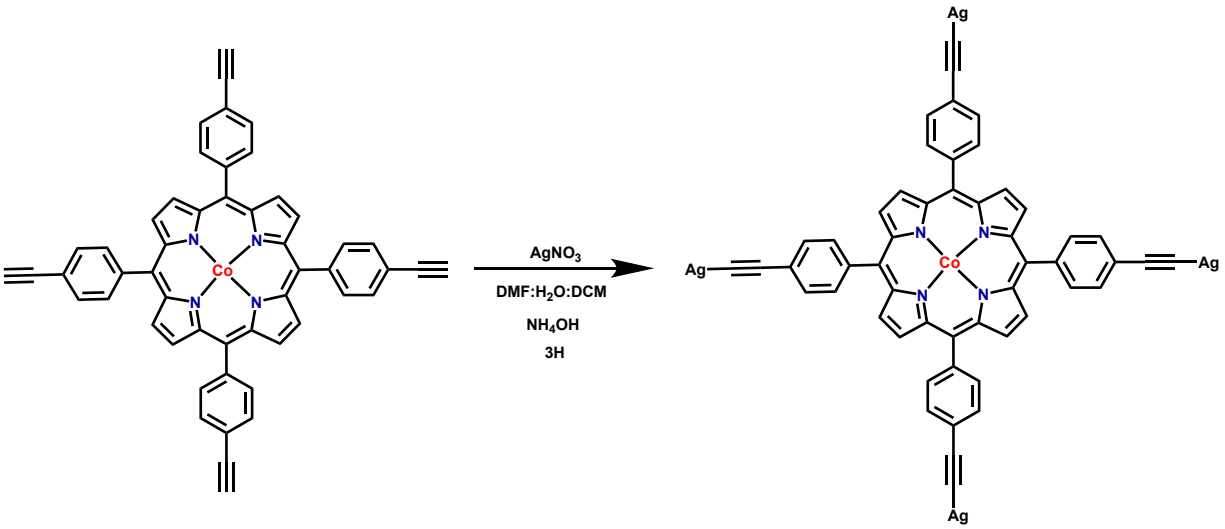

$AgNO_3$ (110.6 mg; 651 µmol; 10 eq) was solubilized in a mixture of MeOH (10 mL) and water (5 mL). To this solution was added NH_4OH until the brown color completely disappeared. CoTATPP (50mg; 65µmol; 1 eq) was dissolved in a mixture of DMF (10mL) and DCM (15mL) and added slowly to the mixture. A precipitate started to form after 10 min and the reaction mixture was stirred at RT for 3H. The solution was filtered and the obtained solid was washed with DMF, water, THF, MeOH and DCM. The resulting dark insoluble solid was obtained quantitatively and dried under vacuum with phosphorus pentoxide overnight.

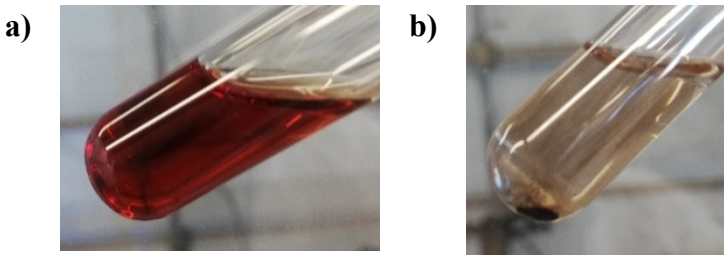

Figure S5 a) C8 solubilised in DCM b) C10 in DCM. A loss of solubility is observed upon silver addition indicative of the complex formation.

C11 [Ag-TaTPP]$_x$

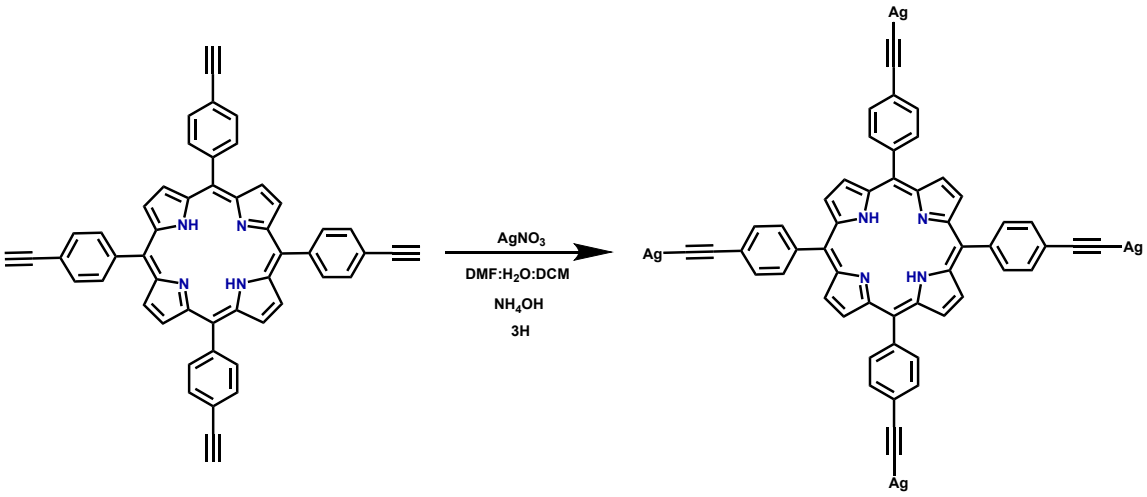

$AgNO_3$ (120.1 mg; 700 µmol) was solubilized in a mixture of MeOH (10 mL) and water (5 mL). To this solution was added NH_4OH until the brown color completely disappeared. TATPP (50mg; 70 µmol; 1 eq) was dissolved in a mixture of DMF (10mL) and DCM (15mL) and added slowly to the mixture. A precipitate started to form after 10 min and the reaction mixture was stirred at RT for 3H. The solution was filtered and the obtained solid was washed with DMF, water, THF, MeOH and DCM. The resulting dark insoluble solid was obtained quantitatively and dried under high vacuum with phosphorus pentoxide overnight.

a) **b)**

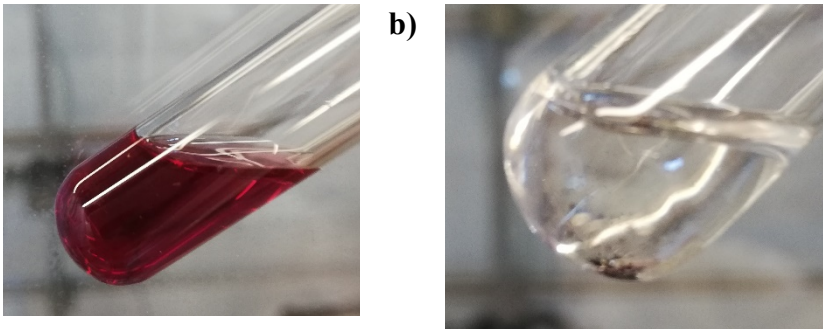

Figure S6 a) C6 solubilised in DCM b) C10 in DCM. A loss of solubility is observed upon silver addition indicative of the complex formation.

Catalysts characterisation

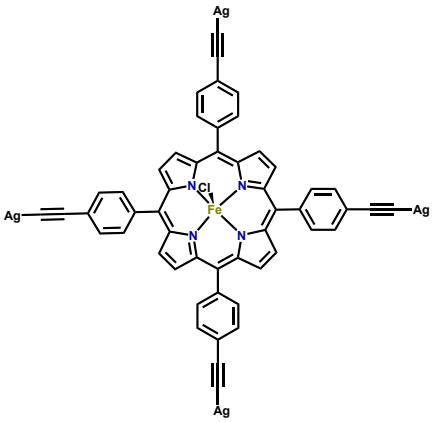

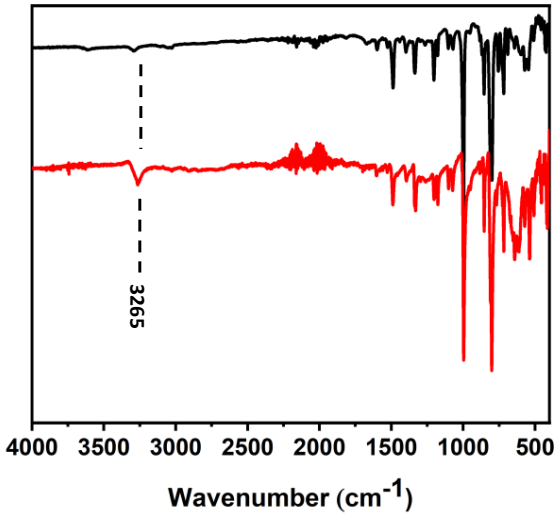

$[Ag\text{-}FeTaTPP]_x$

Figure S7 IR spectrum of compound C9 (Black) and its starting material C7 (red). The intensity of the C≡C-H band (3265 cm^{-1}) is decreased significantly from C7 to C9 upon addition of silver indicative of the C≡C-Ag bond formation. The highlighted peaks are assigned to the C-H stretching of the acetylene and the peaks

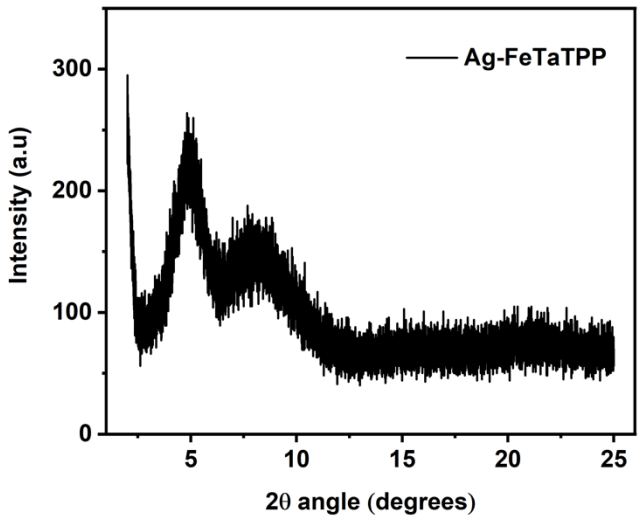

Figure S8: Powder XRD pattern of $[Ag\text{-}FeTaTPP]_x$ between 2 and 25°. The starting material is not crystalline. The observed peaks are of low intensity hinting for a poorly crystalline final structure with a COF-like arrangement. Crystallinity is measured to be 66% (obtained by comparing the integrated intensity of the background with the peaks). Crystal size is calculated to be 83 Å by Scherrer equation.

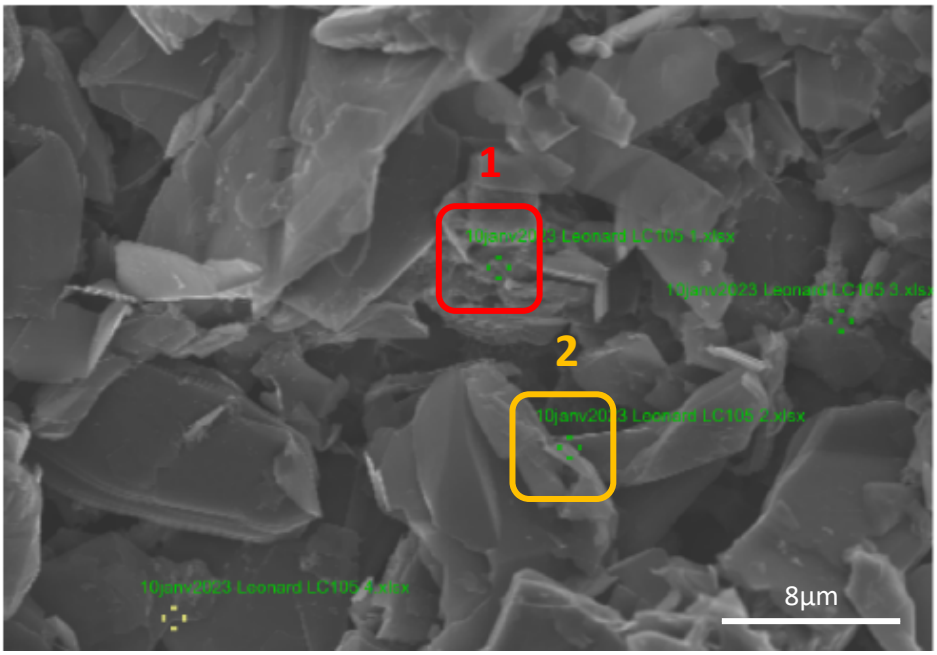

1

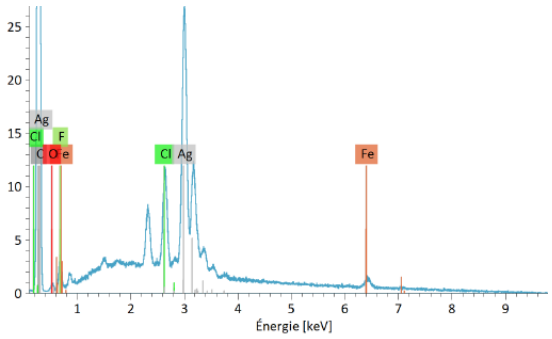

Elément	A	Raies	Net	Mass. [%]	Mass. norm. [%]	Atom. [%]
carbone	6	K	291991	26.73	41.75	81.68
oxygène	8	K	718	0.14	0.21	0.31
fluor	9	K	7400	0.93	1.45	1.80
chlore	17	K	33052	2.89	4.51	2.99
fer	26	K	5656	5.92	9.24	3.89
argent	47	L	173619	27.42	42.83	9.33
			Total	**64.02**	**100.00**	**100.00**

2

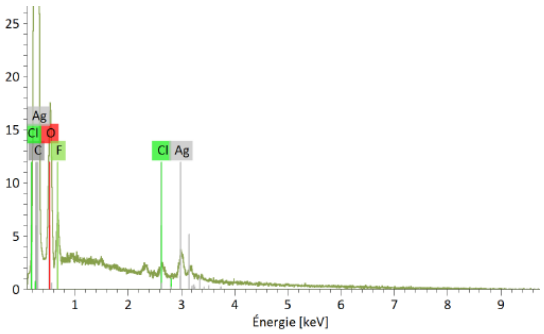

Elément	A	Raies	Net	Mass. [%]	Mass. norm. [%]	Atom. [%]
carbone	6	K	875158	---	90.41	94.24
oxygène	8	K	20687	---	5.84	4.57
fluor	9	K	7604	---	1.29	0.85
chlore	17	K	1821	---	0.26	0.09
argent	47	L	8515	---	2.21	0.26
				Total	**100.00**	**100.00**

Figure S9*:* SEM Picture of a prepared $[Ag\text{-}FeTaTPP]_x$ Electrode. 1 and 2 show quantitative elemental measurements by EDS of $[Ag\text{-}FeTaTPP]_x$ containing spot and without catalyst respectively. Material concentration seems to be highly localized (consequently poorly dispersed) and corresponds to the charging parts of the electrode.

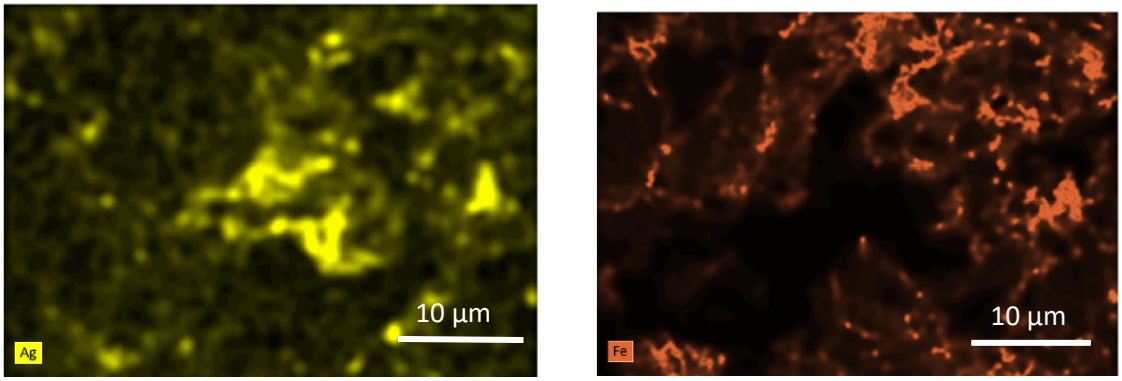

Figure S10*:* SEM-EDS Pictures of Iron and Silver of a prepared $[Ag\text{-}FeTaTPP]_x$ Electrode at 5000x magnification. Fe and Ag signals intensity correspond to charging amorphous particles which we assume to be the chemical of interest confirming the poor catalyst distribution on the electrode.

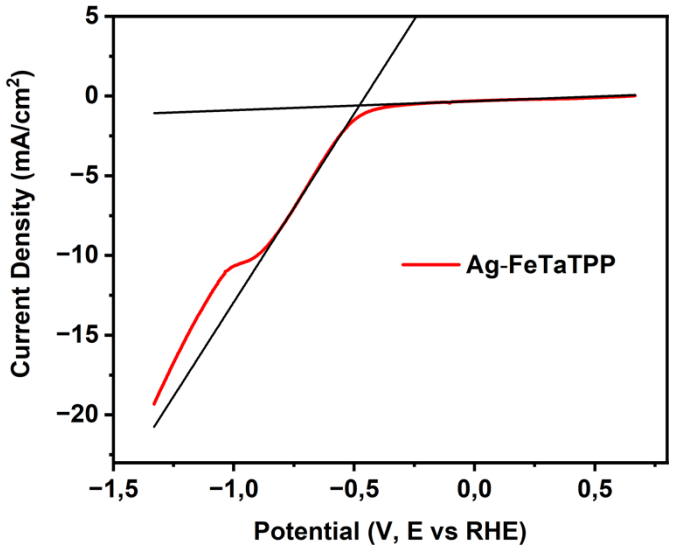

Figure S11: LSV measurement at 10 mV/s (2nd scan) of the deposited $[Ag\text{-}FeTaTPP]_x$ in a 0.5 M $KHCO_3$ solution. Potential is uncorrected. The overpotential is measured as -0.478 V vs RHE as the cross point of the coulombic and faradic currents.

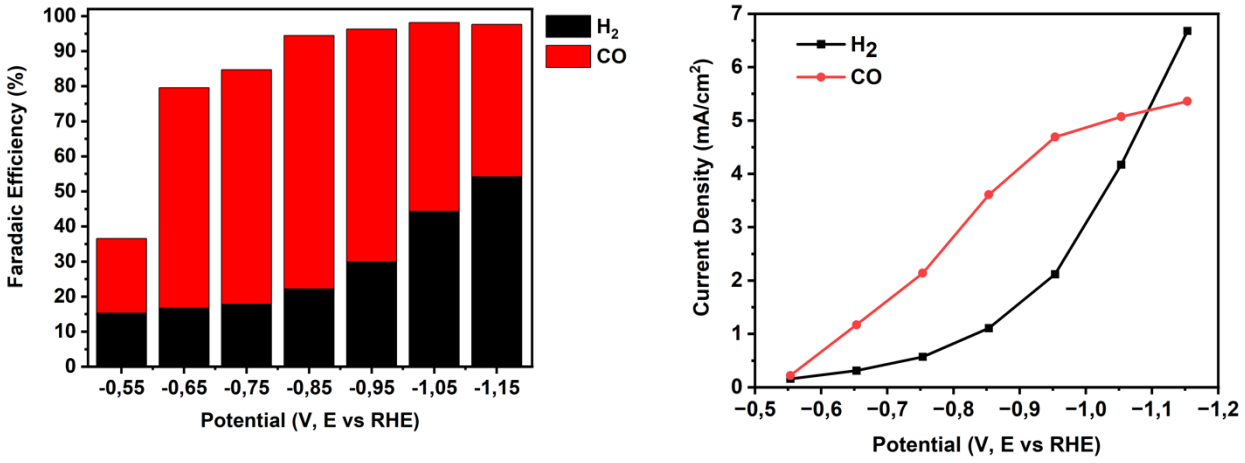

Figure S12: a) [Ag-FeTaTPP]$_x$ measured faradaic efficiency (FE) from direct GC quantification at potential varied between -0.55 and -1.15 V vs RHE in a 0.5 M $KHCO_3$ solution. Potential is uncorrected **b)** Measured current densities for CO and H_2 with varying potential.

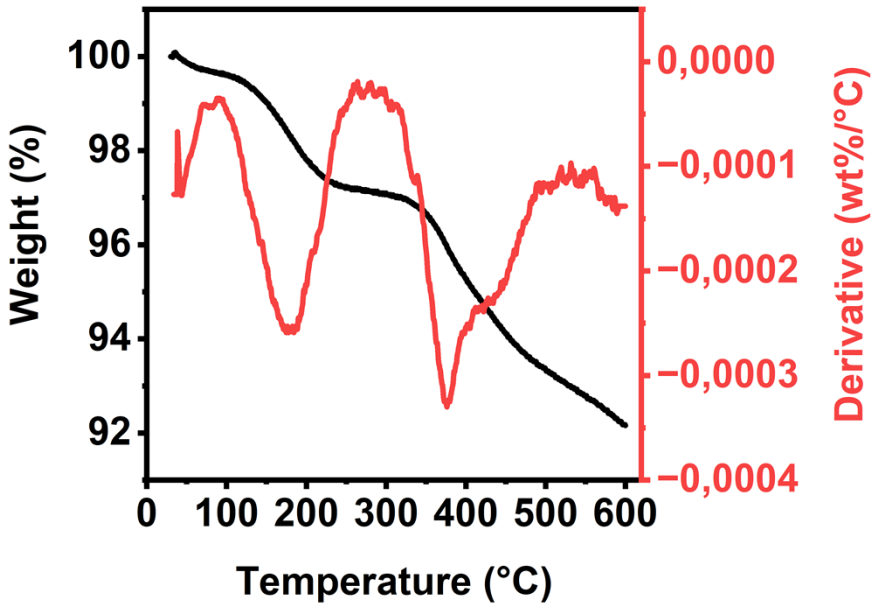

Figure S13: TGA measurement of [FeTaTPPAg]$_x$. The derivative shows two main weight loss steps at 174°C and 376°C.

$[Ag\text{-}CoTaTPP]_x$

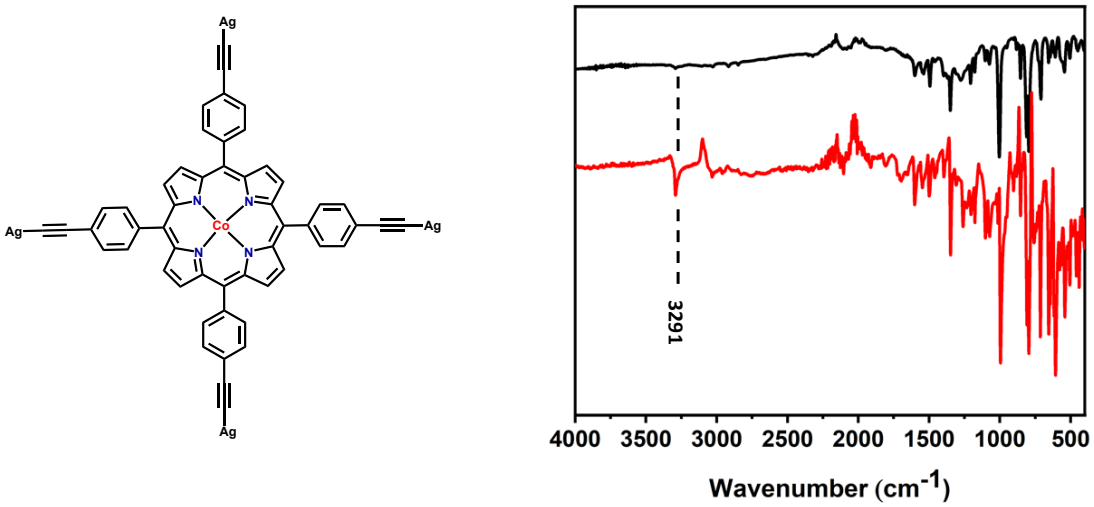

Figure S14 IR spectrum of compound C10 (Black) and its starting C8 (red). The intensity of the C≡C-H band (3291 cm^{-1}) is decreased significantly from C8 to C10 due to the addition of the silver. The highlighted peaks are assigned to the C-H stretching of the acetylene and the peaks

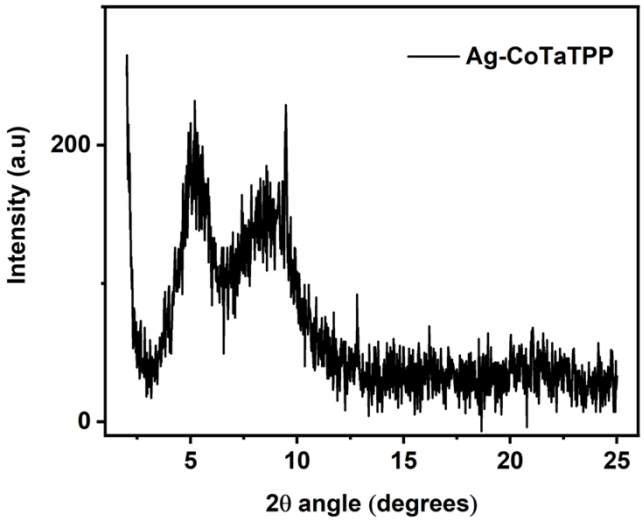

Figure S15*:* Powder XRD pattern of $[Ag\text{-}CoTaTPP]_x$ between 2 and 25°. The starting material is crystalline. The observed peaks are of low intensity hinting for a poorly crystalline final structure with a COF-like arrangement. Crystallinity is measured to be 61% (obtained by comparing the integrated intensity of the background with the peaks). Crystal size is calculated to be 95 Å by Scherrer equation.

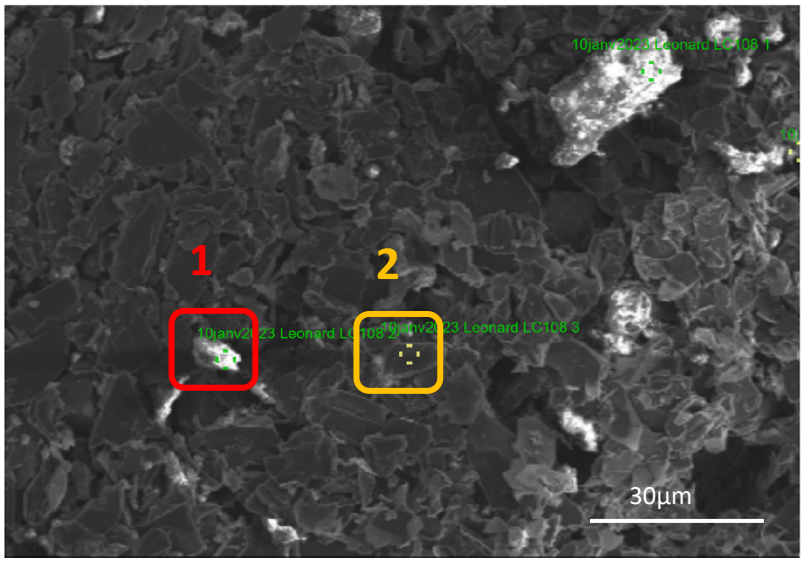

1

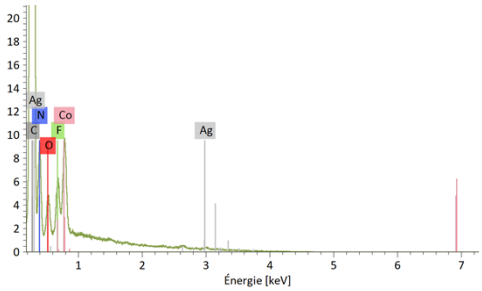

Elément	A	Raies	Net	Mass. [%]	Mass. norm. [%]	Atom. [%]
carbone	6	K	803865	---	81.00	87.98
azote	7	K	26858	---	8.89	8.28
oxygène	8	K	9554	---	1.75	1.43
fluor	9	K	9596	---	1.41	0.97
cobalt	27	L	36079	---	5.03	1.11
argent	47	L	1034	---	1.93	0.23
				Total	**100.00**	**100.00**

2

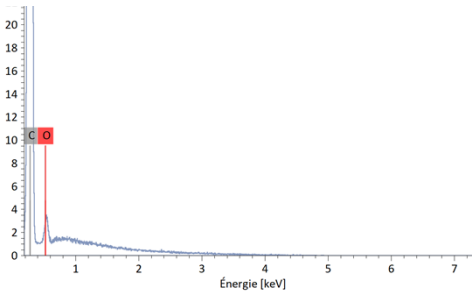

Elément	A	Raies	Net	Mass. [%]	Mass. norm. [%]	Atom. [%]
carbone	6	K	986959	---	98.95	99.21
oxygène	8	K	5440	---	1.05	0.79
				Total	**100.00**	**100.00**

Figure S16*:* SEM Picture of a prepared $[Ag\text{-}CoTaTPP]_x$ Electrode. 1 and 2 show quantitative elemental measurements by EDS of $[Ag\text{-}CoTaTPP]_x$ containing spot and without catalyst respectively. Material concentration seems to be highly localized (consequently poorly dispersed) and corresponds to the charging parts of the electrode.

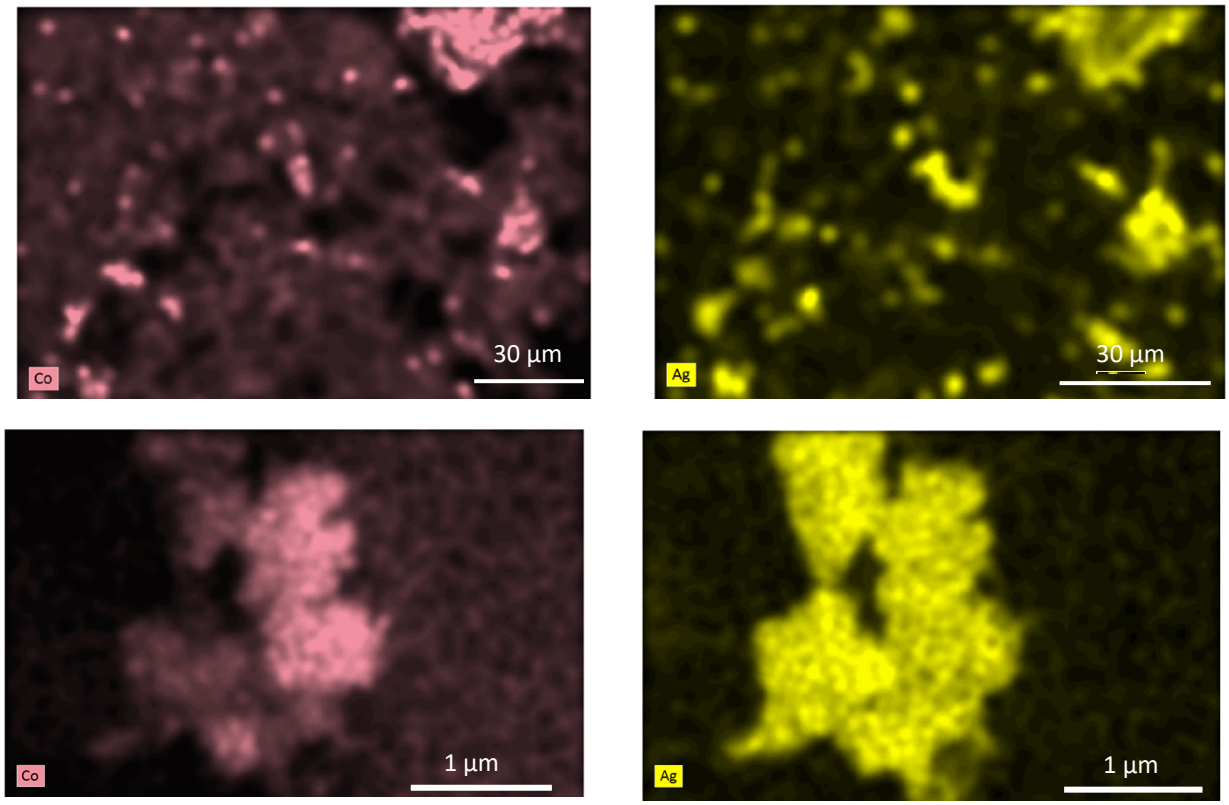

Figure S17: SEM-EDS Pictures of Cobalt and Silver of a prepared $[Ag\text{-}CoTaTPP]_x$ Electrode at 1500x and 50 000x magnification. Co and Ag signals intensity correspond to charging amorphous particles which we assume to be the chemical of interest confirming the poor catalyst distribution on the electrode.

Figure S18: LSV measurement at 10 mV/s (2nd scan) of the deposited $[Ag\text{-}CoTaTPP]_x$ in a 0.5 M $KHCO_3$ solution. Potential is uncorrected. The overpotential is measured as -0.409 V vs RHE as the cross point of the coulombic and faradic currents.

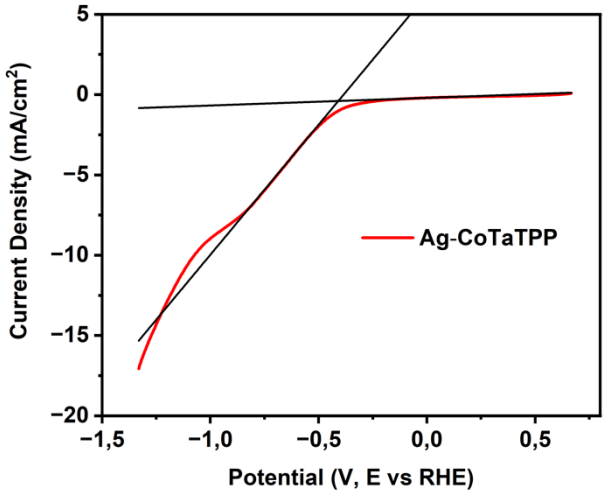

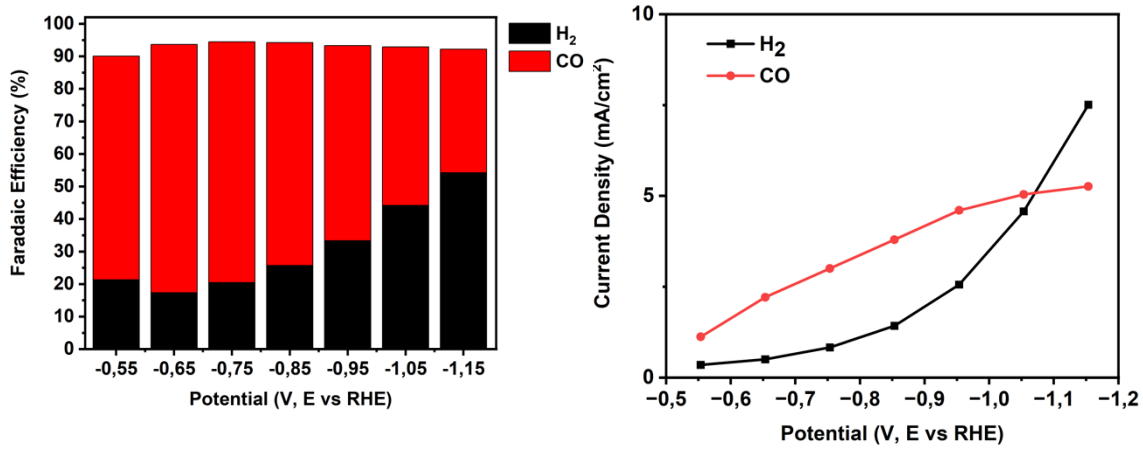

Figure S19: a) [Ag-CoTaTPP]$_x$ measured faradaic efficiency (FE) from direct GC quantification at potential varied between -0.55 and -1.15 V vs RHE in a 0.5 M $KHCO_3$ solution. Potential is uncorrected **b)** Measured current densities for CO and H_2 with varying potential.

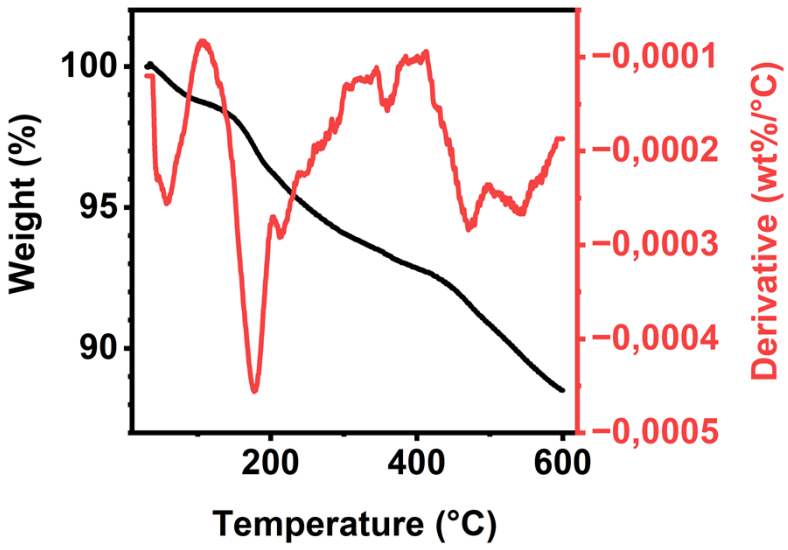

Figure S20: TGA measurement of [CoTaTPPAg]$_x$. A first step at low temperature is assumed to be a solvent evaporation. The derivative shows two main weight loss steps at 179°C and 475-542°C.

$[Ag\text{-}TaTPP]_x$

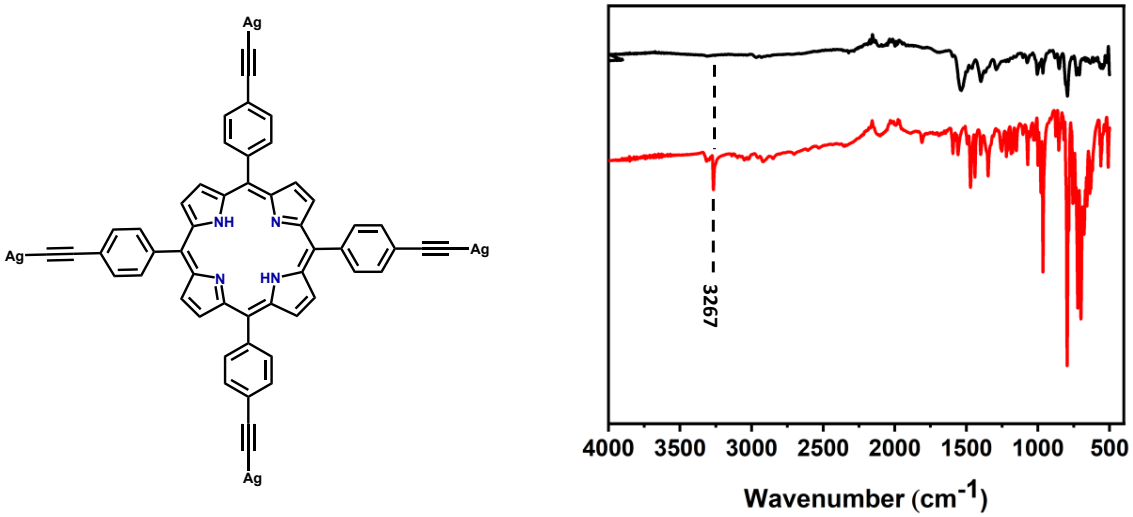

Figure S21 IR spectrum of compound C11 (Black) and its starting C6 (red). The intensity of the C≡C-H band (3267 cm^{-1}) is decreased significantly from C6 to C11 due to the addition of the silver. The highlighted peaks are assigned to the C-H stretching of the acetylene and the peaks

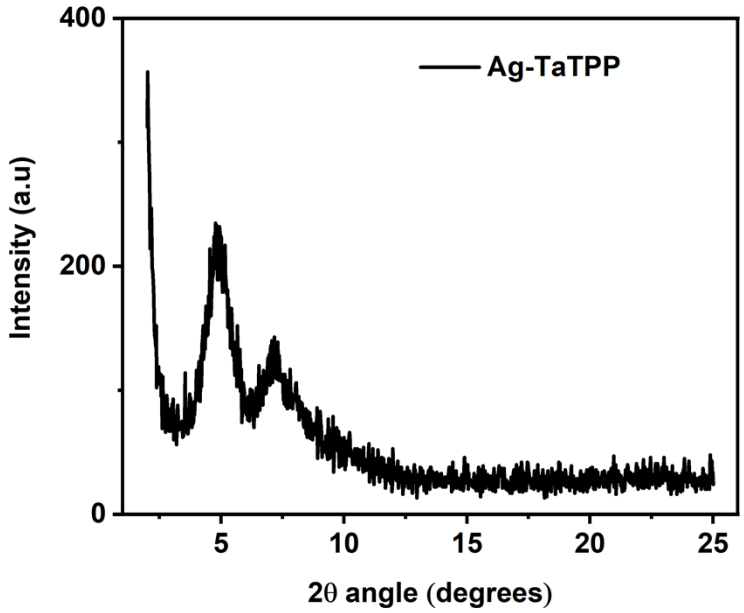

Figure S22*:* Powder XRD pattern of $[Ag\text{-}TaTPP]_x$ between 2 and 25°. The starting material is amorphous. The observed peaks are of low intensity hinting for a poorly crystalline final structure with a COF-like arrangement. Crystallinity is measured to be 68% (obtained by comparing the integrated intensity of the background with the peaks). Crystal size is calculated to be 115 Å by Scherrer equation.

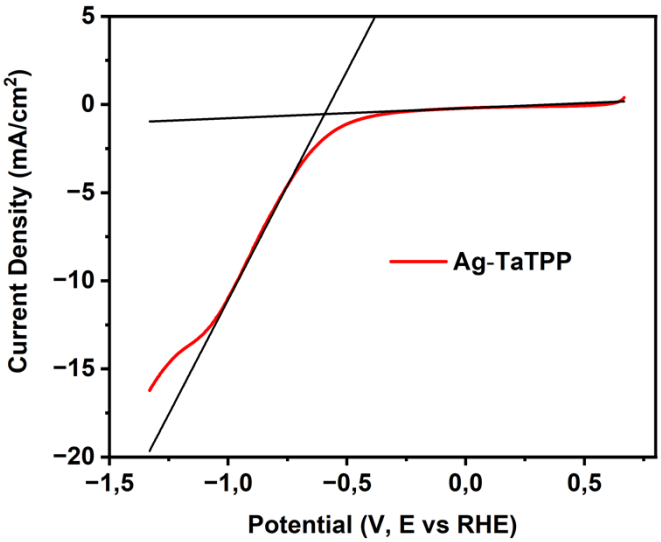

Figure S23: LSV measurement at 10 mV/s (2nd scan) of the deposited $[Ag\text{-}TaTPP]_x$ in a 0.5 M $KHCO_3$ solution. Potential is uncorrected. The overpotential is measured as -0.59427 V vs RHE as the cross point of the coulombic and faradic currents

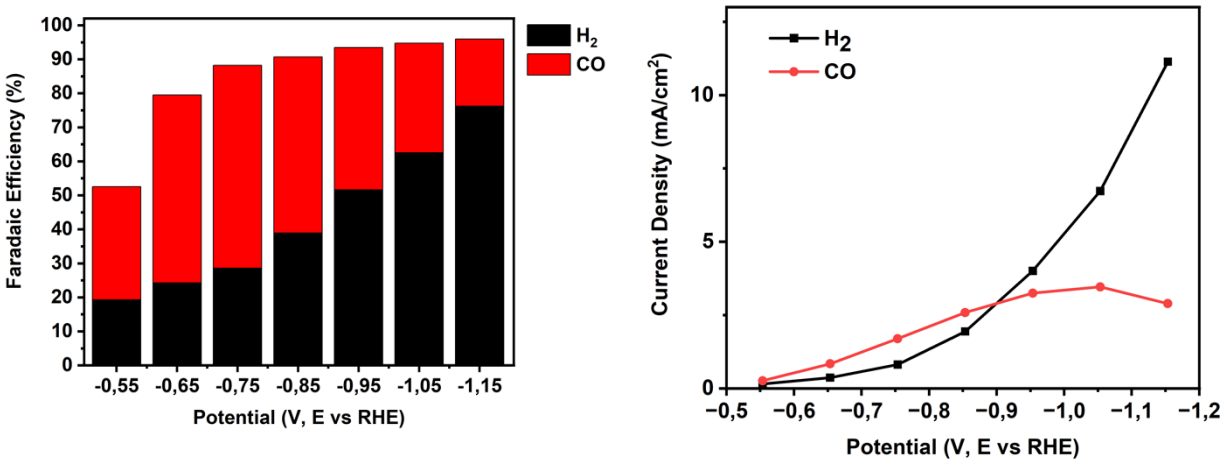

Figure S24: a) $[Ag\text{-}TaTPP]_x$ measured faradaic efficiency (FE) from direct GC quantification at potential varied between -0.55 and -1.15 V vs RHE in a 0.5 M $KHCO_3$ solution. Potential is uncorrected **b)** Measured current densities for CO and H_2 with varying potential.

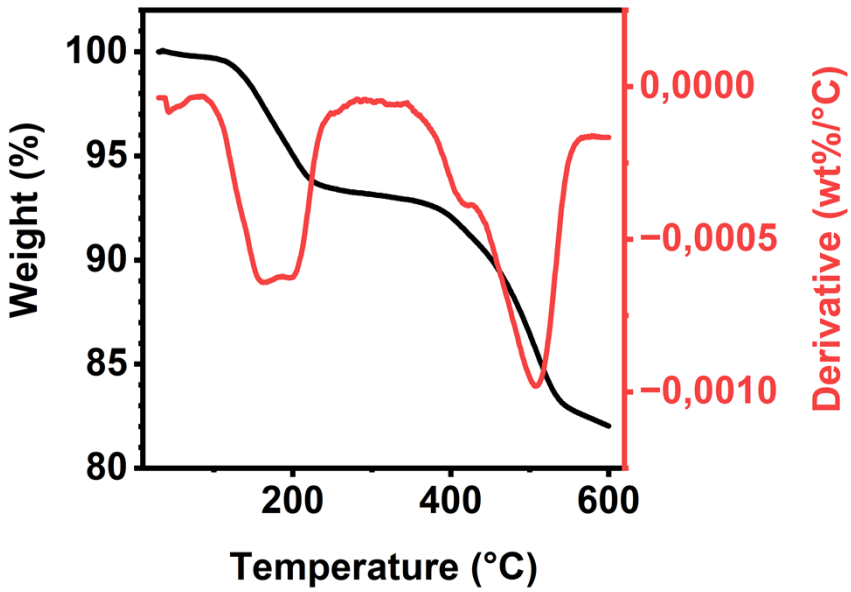

Figure S25: TGA measurement of $[TaTPPAg]_x$. The derivative shows 3 main weight loss steps at 161°C, 198°C and 507°C

Comparative graphs

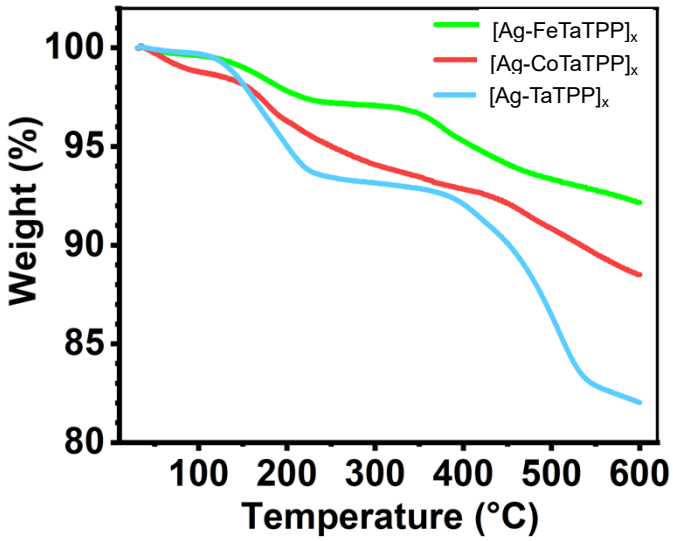

Figure S26: TGA measurement comparison for the derivatives. The mass loss is more important for the unmetalled porphyrin but a similar decomposition pattern is observed in every case with a first mass loss between 160 and 200°C followed by a second step.

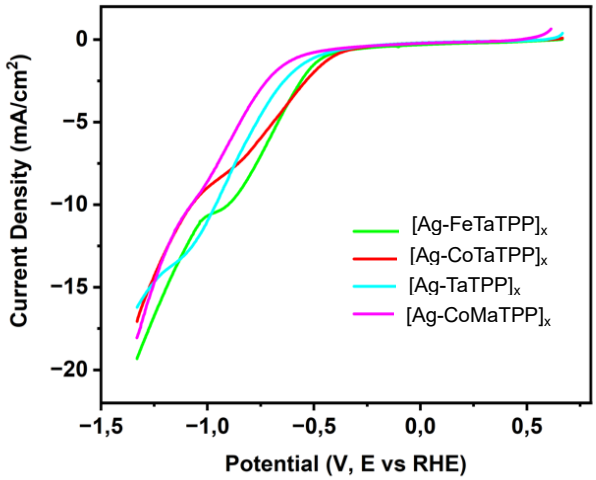

Figure S27: LSV comparison at 10 mV/s of the deposited materials in a 0.5 M $KHCO_3$ solution. Potential is uncorrected.

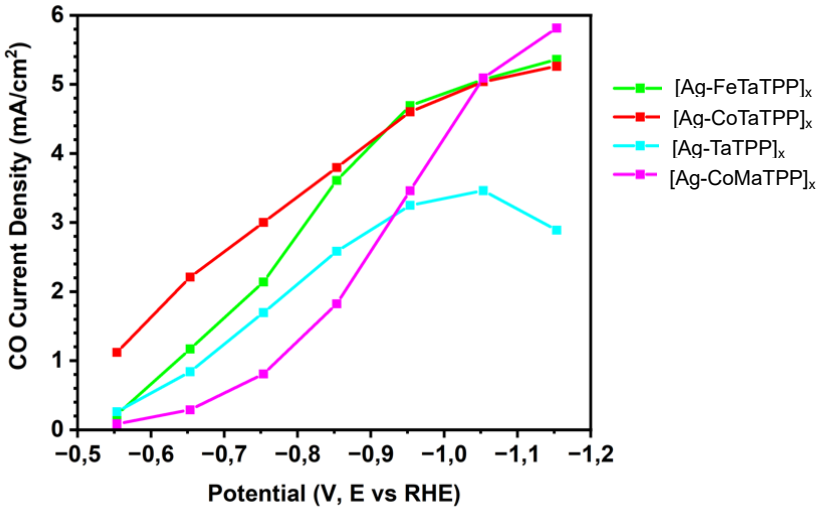

Figure S28: Current density comparison at varying potential of the deposited materials in a 0.5 M $KHCO_3$ solution. Potential is uncorrected. [Ag-TaTPP]x activity for CO reaches a plateau (corresponding to H_2 evolution increase) while the presence of metalated porphyrins are delaying this effect.

X-Ray photoelectron spectroscopy (XPS)

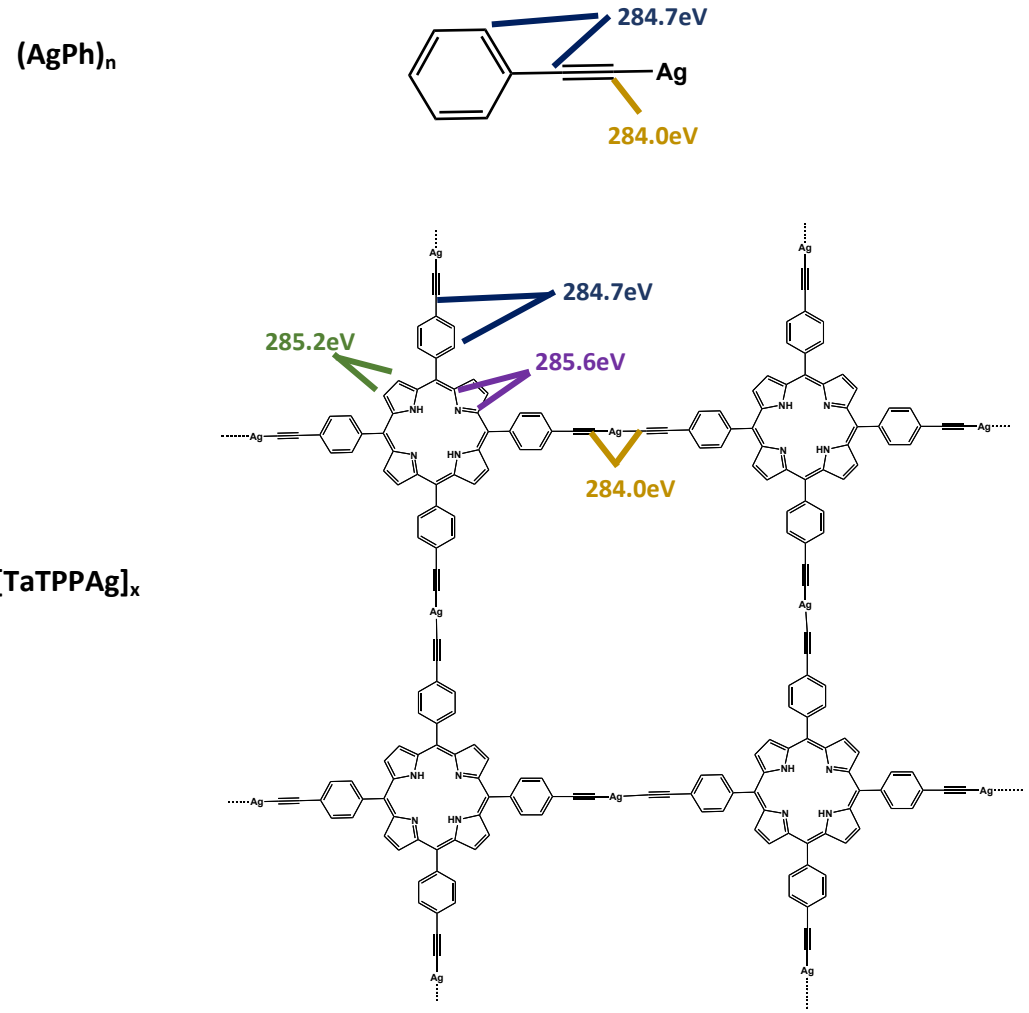

Figure S29*:* XPS identification and attribution of the carbon chemical environments in the chemical structure. The Identification of all the chemical environments was achieved via comparison with a reference silver acetylide (AgPh)n of known structure and the corresponding porphyrin starting material (tetra acetylene Fe-porphyrin) and un-metalated porphyrin. Further peak deconvolution on the $[TaTPPAg]_x$ allowed identifying characteristic bonds features.

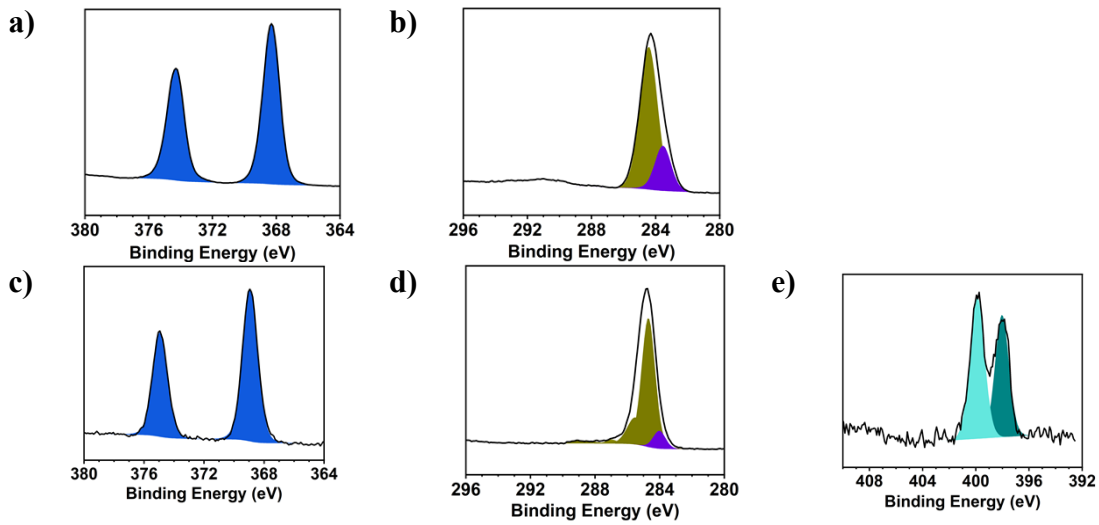

Figure S30*:* XPS measurements for a reference compound AgPh (**a-b**) and $[Ag\text{-}TaTPP]_x$ (**c-e**). **a)** Ag3d spectrum of the reference compound **b) c)** Ag3d spectrum shows an Ag(I) species (Ag3d 1/2 (375 eV) Ag3d 3/2 (369 eV). **d)** C1s deconvolution shows a maintained porphyrin structure (Pyrrole band (285.2 and 285.6 eV) and Phenyl band (284.7 eV) with a component at 284 eV attributed to the Ag-C≡C bond. **e)** N1s shows 2 bands corresponding to the N-H (399.9eV) and N (398 eV) of the free base porphyrin.

Table S1 Elemental XPS measurement. The value Ag/acetylene corresponds to the ratio of total silver integration over the N content (assumed to be only present on the porphyrin core)

	C	O	N	Fe	Cl	Ag	Ag/acetylene
$(AgPh)_n$	84	1.5				15	
$[TaTPPAg]_x$	67	15	2.2			2,.	1.23
$[FeTaTPPAg]_x$	80	7.1	4.8	1.3	0.8	5.2	1.08

Single crystal X-Ray diffraction structure

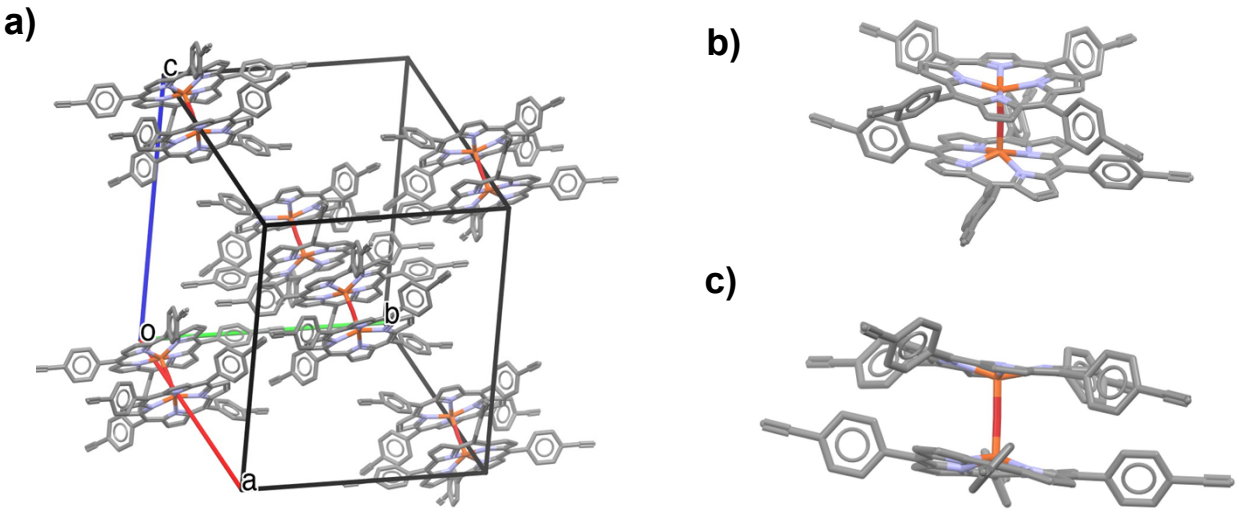

Figure S31: X-Ray diffraction single crystal structure of the Oxygen-bridged porphyrin dimer; a) unit cell view of the dimers' packing arrangement; b view of the dimer; c) and b) side view of the dimer.

Figure S32: X-Ray diffraction single crystal structure of the Oxygen-bridged porphyrin dimer; a) top view of the dimer in ellipsoid style with 50% probability level b) side view of the dimer in ellipsoid style with 50% probability level

Mass spectrometry

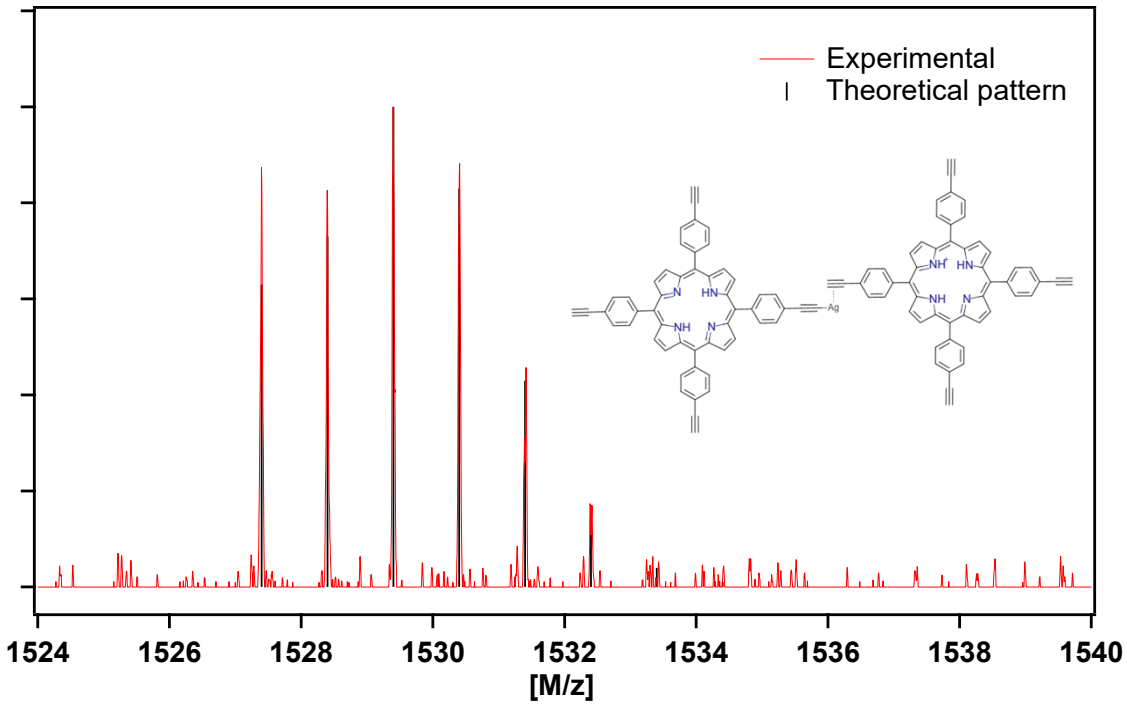

Figure S33: Mass spectrum (MALDI TOF) of $[TaTPPAg]_x$ showing a mass pattern corresponding to a dimeric fragment of the cluster.